References

1. Conneely OM. Antiinflammatory activities of lactoferrin. J Am Coll Nutr 2001;20(5 suppl):389S–95S.
2. Brock JH. Lactoferrin: an overview of research and prospects. Milk Sci 2004;53:219–25.
3. Danjo Y, Lee M, Horimoto K, Hamano T. Ocular surface damage and tear lactoferrin in dry eye syndrome. Acta Ophthalmol (Copenh) 1994;72:433–7.
4. Pflugfelder SC, Jones D, Ji Z, et al. Altered cytokine balance in the tear fluid and conjunctiva of patients with Sjögren's syndrome keratoconjunctivitis sicca. Curr Eye Res 1999;19: 201–11.
5. Fujihara T, Nagano T, Nakamura M, Shirasawa E. Lactoferrin suppresses loss of corneal epithelial integrity in a rabbit short-term dry eye model. J Ocul Pharmacol Ther 1998;14:99–107.
6. Chow SC, Liu JP. Sample size determination. In: Balding DJ, Noel AC, eds. Design and Analysis of Clinical Trials. Concept and Methodologies. Hoboken, NJ: Wiley Interscience; 2004:438–510.

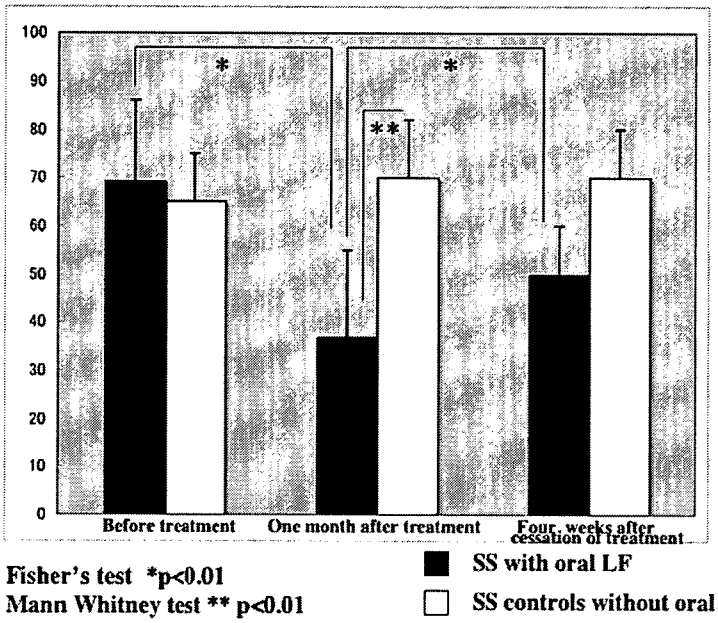

Figure 1. Change in mean visual analog ocular symptom (VAS) score with lactoferrin (LF) treatment. Note the significant decrease in the mean VAS score with 1 month of lactoferrin use and the reincrease in the mean score 4 weeks after cessation of treatment. SS = Sjögren's syndrome.

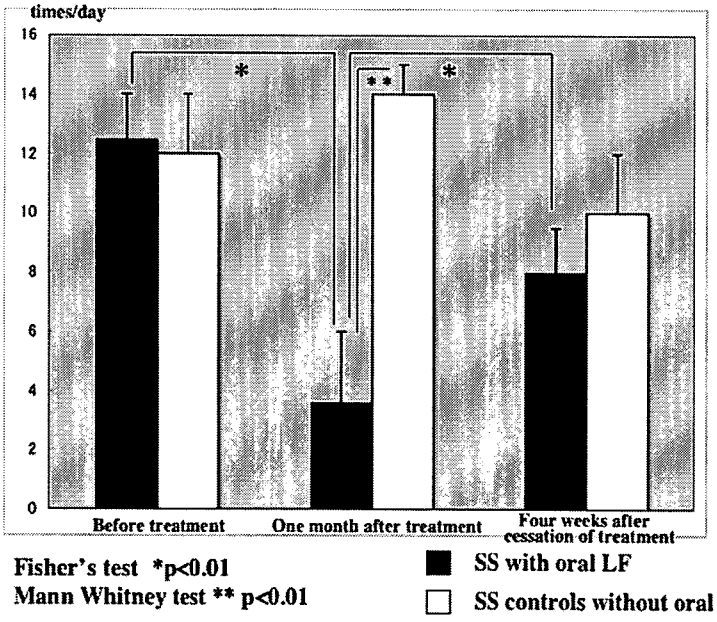

Figure 2. Change in frequency of artificial tear drop instillations per day with lactoferrin (LF) treatment. Note the significant decrease in the mean number of artificial tear drop instillations with 1 month of lactoferrin use and the reincrease in the frequency of instillations 4 weeks after cessation of treatment. SS = Sjögren's syndrome.

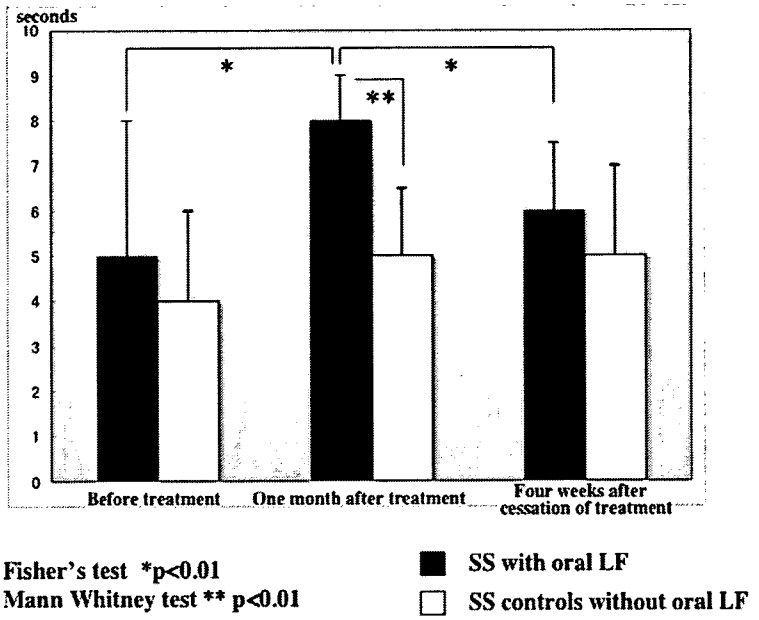

Figure 3. Change in mean tear film breakup time (BUT) values with lactoferrin (LF) treatment. Note the improvement of the tear film BUT with 1 month of lactoferrin use and the deterioration of tear stability 4 weeks after cessation of treatment. SS = Sjögren's syndrome.

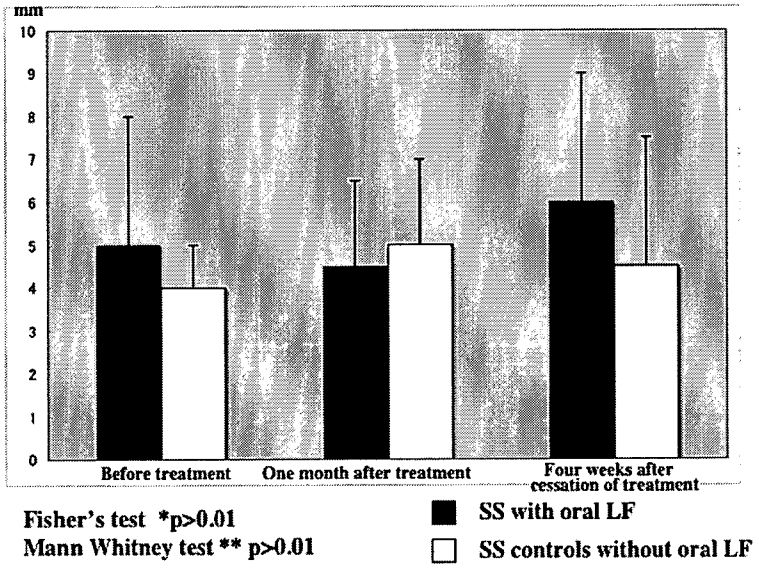

Figure 4. Change in mean Schirmer test scores with lactoferrin (LF) treatment. Note the absence of statistically significant changes in tear quantity with lactoferrin use or its withdrawal. SS = Sjögren's syndrome.

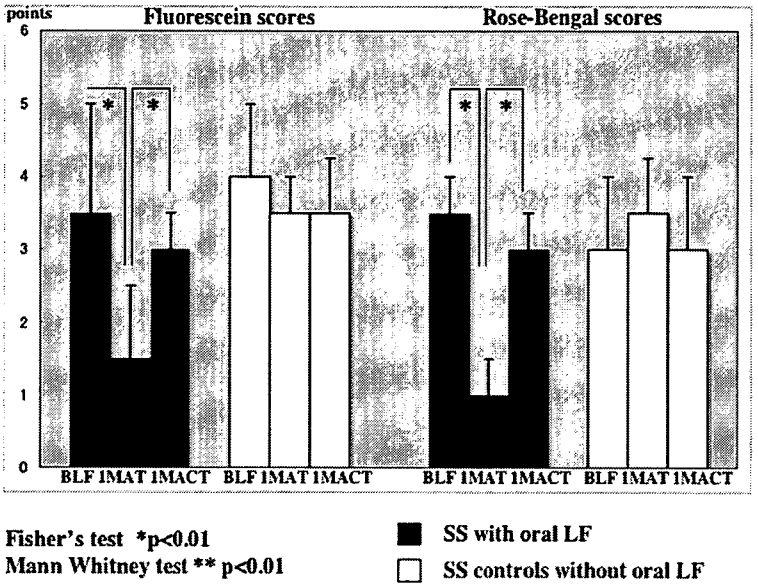

Figure 5. Change in mean vital staining scores with lactoferrin (LF) treatment. Note the significant improvements of the ocular surface vital staining scores with 1 month of lactoferrin use and the deterioration with cessation of lactoferrin. 1MACT = 1 month after cessation of treatment; 1MAT = 1 month after treatment; BLF = before lactoferrin treatment; SS = Sjögren's syndrome.

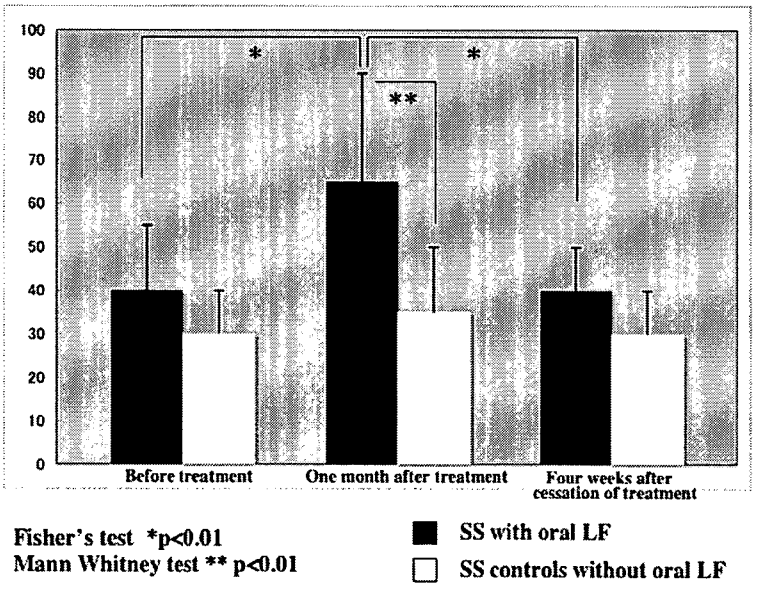

Figure 6. Change in mean tear film lipid layer thickness with lactoferrin (LF) treatment. Note the significant improvement of the mean tear film lipid layer thickness with 1 month of lactoferrin use and the deterioration with cessation of lactoferrin. SS = Sjögren's syndrome.

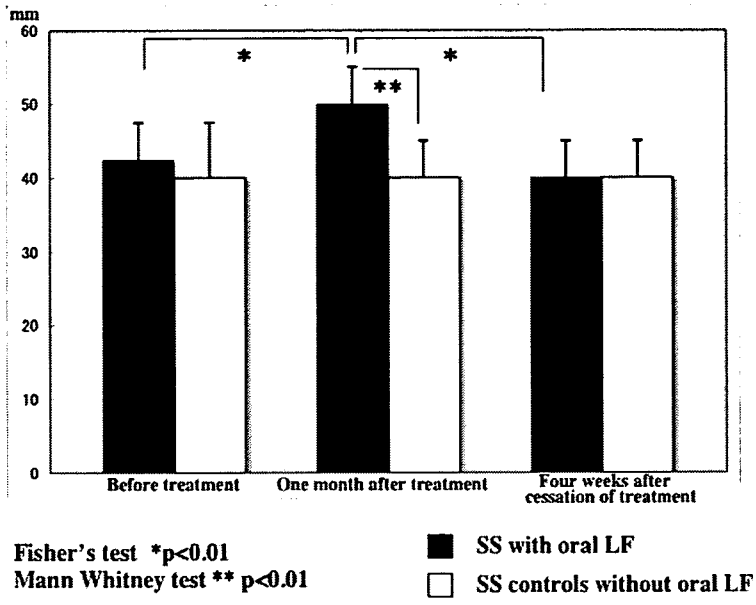

Figure 7. Change of mean corneal sensitivity with lactoferrin (LF) treatment. Note the significant improvement of the mean corneal sensitivity with 1 month of lactoferrin use and its significant deterioration with cessation of lactoferrin. SS = Sjögren's syndrome.

Impression cytology parameters	Before LF treatment	One month after LF treatment	Four weeks after cessation of treatment
Squamous Metaplasia (Nelson's Grade)	2.0±0.5	1.00±0.64 *	1.75±0.25 *
Goblet cell density (cells/mm²)	385±100	912±50 *	426±180 *

Figure 8. Impression cytology parameters. Note the significant improvements of the mean squamous metaplasia grade and goblet cell density with 1 month of lactoferrin (LF) use and the deterioration with cessation of lactoferrin. *$P<0.01$, Fisher exact test.

Tear Evaporation Rates in Sjögren Syndrome and non-Sjögren Dry Eye Patients

EIKI GOTO, YUKIHIRO MATSUMOTO, MIZUKA KAMOI, KOJI ENDO, REIKO ISHIDA, MURAT DOGRU, MINAKO KAIDO, TAKASHI KOJIMA, AND KAZUO TSUBOTA

• PURPOSE: To reinvestigate tear evaporation rates in Sjögren syndrome (SS) and non-Sjögren (non-SS) dry eye patients with a recently reported ventilated chamber evaporimeter system.

• DESIGN: Prospective case-control study.

• METHODS: A ventilated chamber evaporimeter system was used to measure tear evaporation rates. A DR-1 camera (Kowa, Nagoya, Japan) was used for tear lipid layer interference image acquisition. The Yokoi severity grading system was used for DR-1 image evaluation. Twenty-four aqueous tear deficiency (ATD) eyes of 21 consecutive patients with SS were studied (SS ATD group). Twenty-one ATD eyes of 12 non-SS patients (non-SS ATD group) were examined as control subjects.

• RESULTS: Tear evaporation rates of the SS ATD group (5.9 ± 3.5 [10^{-7} g/cm^2 per second]) were significantly higher than those of the non-SS ATD group (2.9 ± 1.8 [10^{-7} g/cm^2 per second]; $P = .0009$). The severity grading of DR-1 tear interference images of the SS ATD group was significantly higher ($P = .03$), along with significantly worse meibomian gland expressibility and vital staining scores, compared with those of the non-SS ATD group.

• CONCLUSIONS: Tear evaporation rates were higher in eyes of the SS ATD group compared with the non-SS ATD group. Tear evaporation assessed in conjunction with tear lipid layer findings and meibomian gland expressibility provides an increased understanding in the differential diagnosis of dry eye states. (Am J Ophthalmol 2007;144:81–85. © 2007 by Elsevier Inc. All rights reserved.)

AFTER THE NATIONAL EYE INSTITUTE REPORT BY Lemp, tear evaporimetry to describe evaporative water loss from the ocular surface has been considered as an important examination to differentiate the types of dry eye in addition to the basic Schirmer I test.[1,2] The ocular surface tear film consists of lipid, aqueous, and mucin layers. The tear film spreads across the ocular surface by blinking and drains mainly into the nasolacrimal duct, with the remainder evaporating into the air. The mucin layer is secreted by the goblet cells and the ocular surface epithelium, aqueous components are secreted from the lacrimal gland, and the lipid layer is formed by secreted meibomian lipids that act to suppress excessive tear evaporation by covering the aqueous tear layer.[3,4]

In dry eye, tear evaporation has been considered to be important because the ratio of tear evaporation in total tear flow is increased compared with that of normal subjects.[5] Previous tear evaporation reports in aqueous tear deficiency (ATD) dry eyes have revealed inconsistent results by several groups, sometimes higher[6,7] or sometimes lower[8–10] than the normal values.

We recently reinvestigated the tear evaporation rates in normal subjects and meibomian gland dysfunction (MGD) patients using the new ventilated chamber evaporimeter system.[11] As the meibomian gland lipid expressibility worsened, tear evaporation rates showed an increase under normal aqueous tear secretion. Thus, we thought that the comparison of tear evaporation rates of ATD dry eyes in patients with and without Sjögren syndrome (SS) were intriguing and warranted further investigation. Herein, we report tear evaporation rates of ATD dry eyes in patients with SS and ATD dry eyes in patients without SS using our new evaporimeter system which uses a ventilated chamber.[11] Tear interferometry to evaluate the precorneal tear lipid layer condition was performed simultaneously using the Yokoi semiquantitative grading system[12,13] and lipid layer thickness quantification system.[14] The significance of this method and findings are discussed.

METHODS

• SUBJECTS: In the subspecialty clinic of Tokyo Dental College, Ichikawa General Hospital, 24 ATD eyes of 21 consecutive patients with SS were studied (SS ATD group: one male and 20 females; mean age, 55.8 ± 13.1 years). Twenty-one ATD eyes of 12 non-SS patients (non-SS ATD group: three males and nine females; mean age, 51.9 ± 17.2 years) were examined as control subjects. SS patients were diagnosed using the criteria of Fox and Saito.[15] The

Accepted for publication Mar 30, 2007.

From the Department of Ophthalmology, School of Dental Medicine, Tsurumi University, Yokohama, Japan (E.G.); the Department of Ophthalmology, School of Medicine, Keio University, Tokyo, Japan (E.G., Y.M., M.K., R.I., M.D., M.K., T.K., K.T.); the Department of Ophthalmology, Ichikawa General Hospital, Tokyo Dental College, Ichikawa, Japan (Y.M., R.I., M.D., M.K., T.K., K.T.); the Analytical Research Center, KAO Corporation, Tochigi, Japan (K.E.); and the Department of Ophthalmology, Social Insurance Chukyo Hospital, Nagoya, Japan (T.K.).

Inquiries to Eiki Goto, Department of Ophthalmology, School of Dental Medicine, Tsurumi University, 2-1-3 Tsurumi, Tsurumi-ku, Yokohama City, Kanagawa, Japan 230-8501; e-mail: goto-e@tsurumi-u.ac.jp

0002-9394/07/$32.00
doi:10.1016/j.ajo.2007.03.055

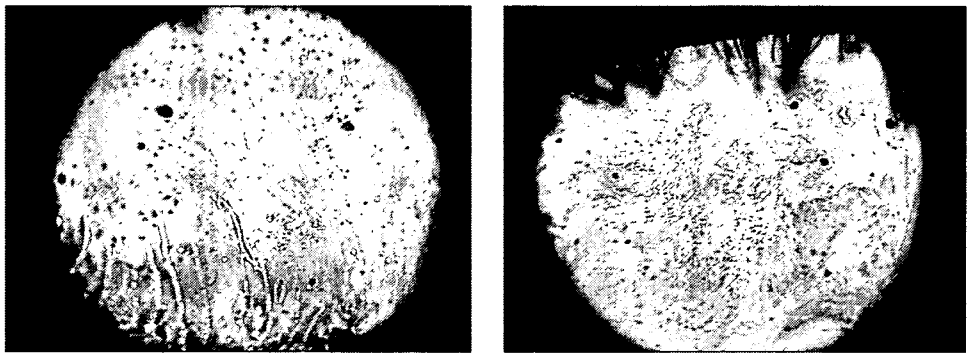

FIGURE. Representative DR-1 tear interference images from the Sjögren syndrome (SS) aqueous tear deficiency (ATD) and the non-SS ATD groups. (Left) Representative DR-1 image from a 65-year-old Asian woman in the SS ATD group. Tear evaporation rates were 5.7 (10^{-7} g/cm^2 per second), the Yokoi DR-1 grading was 4, and the range of lipid layer thickness estimated from the DR-1 tear interference image was 40 to 240 nm. Fluorescein and rose bengal scores were 6 and 5, respectively. The tear break-up time (BUT) was one second, the Schirmer I test value was 3 mm, and meibomian gland expressibility grading was 3. (Right) Representative DR-1 image from a 73-year-old Asian woman in the non-SS ATD group. Tear evaporation rates were 1.1 (10^{-7} g/cm^2 per second), the Yokoi DR-1 grading was 4, and the range of lipid layer thickness estimated from the DR-1 tear interference image was 120 to 220 nm. Fluorescein and rose bengal scores were 5 and 4, respectively. The tear BUT was four seconds, the Schirmer I test value was 2 mm, and meibomian gland expressibility grading was 2.

Japanese diagnostic criteria of dry eye was used for the diagnosis of dry eye, and Schirmer I test results of 5 mm or less were regarded as ATD.[16] Both eyes of all subjects underwent measurement. Only those eyes with Schirmer I test results of 5 mm or less were included as ATD eyes in this study. None of the subjects had any evidence of ocular infection, none wore contact lenses, none had undergone punctal occlusion, and none had blepharospasm, conjunctivochalasis, or abnormal blinking. Severe dry eye states, such as Stevens-Johnson syndrome or ocular pemphigoid, and cases with allergic conjunctivitis were excluded from the study.

• TEAR EVAPORIMETER SET UP: Tear evaporation rates from the ocular surface were measured noninvasively using our recently reported device.[11] Briefly, the evaporimeter consisted of an eye cup in the form of a ventilated chamber having a volume of 20 cm^3 that tightly covered the eye; air, which was supplied into the cup as a tear evaporation carrier by an air compressor at a constant flow rate (150 ml/minute), and a quartz crystal sensor (9 MHz A-T cut quartz crystal 8 mm in diameter and 0.2 mm in thickness), known as the microbalance, which is highly sensitive to humidity. The frequency of the sensor shifts in response to changes in humidity. Evaporation rates were measured by calculating the difference between the water content of the air entering and exiting the cup. The data sampling rate was four times per second. Real-time changes in the frequency data appeared on the display of a personal computer, synchronous with this sampling rate. For the measurement, the same eye cup was used as in the previous study to fix the condition.[11]

• EXAMINATIONS OF TEARS, THE OCULAR SURFACE, AND MEIBOMIAN GLANDS: Tear lipid layer interferometry was performed noninvasively after tear evaporimetry using the DR-1 camera system[12] (Kowa, Nagoya, Japan) before any invasive examination. DR-1 tear interference images were recorded using a digital photo printer, and the evaluation of tear interference images was carried out using the Yokoi semiquantitative dry eye severity grading system as reported previously: grade 1, somewhat gray color, uniform distribution; grade 2, somewhat gray color, nonuniform distribution; grade 3, a few colors, nonuniform distribution; grade 4, many colors, nonuniform distribution; grade 5, corneal surface partially exposed. In their report, normal control eyes were classified into grades 1 and 2 and dry eyes were classified into grades 2, 3, 4, and 5.[12,13] For the most recent data from 16 eyes of eight patients (six eyes of three SS patients, and 10 eyes of five non-SS patients), DR-1 images were acquired using the uncompressed high-quality image capturing system,[17,18] and tear lipid layer thickness was quantified using a computer-synthesized interference color chart system in the representative cases.[14]

Examination of the ocular surface was performed identically as in a previous report using the new tear evaporimetry.[11] Briefly, the ocular surface was examined by the double-staining method with 2 μl preservative-free solution consisting of 1% fluorescein and 1% rose Bengal dye. Fluorescein and rose bengal staining scores (minimum, zero; maximum, nine) and tear break-up times (BUT) were recorded.[19,20] The Schirmer I test also was performed. To assess meibomian gland expressibility, the Shimazaki grading system was used.[9] Digital pressure was applied on the lower tarsus, and the degree of ease of expression of

TABLE. Comparison of Tear Evaporimetry, Tear Interferometry, and Ocular Signs between the Sjögren Syndrome Aqueous Tear Deficiency and non-Sjögren Syndrome Aqueous Tear Deficiency Groups

	Tear Evaporation Rates (10^{-7} g/cm^2 per second)	DR-1 Grading (1–5)	Fluorescein Staining Score (0–9)	Rose Bengal Staining Score (0–9)	Tear BUT (sec)	Schirmer I Test Value (mm)	Meibomian Gland Expressibility (0–3)
SS ATD (n = 24)	5.9 ± 3.5	3.9 ± 1.2	3.0 ± 2.4	3.7 ± 2.6	2.6 ± 1.7	2.5 ± 2.0	2.2 ± 0.4
Non-SS ATD (n = 21)	2.9 ± 1.8	2.9 ± 1.1	0.9 ± 1.6	1.9 ± 2.5	3.1 ± 2.6	2.0 ± 2.0	1.0 ± 1.3
P value	.0009	.03	.002	.01	.95	.3	.04

ATD = aqueous tear deficiency; BUT = tear break-up time; SS = Sjögren syndrome.

meibomian secretions was evaluated semiquantitatively as follows: grade 0, clear fluid easily expressed; grade 1, cloudy fluid expressed with mild pressure; grade 2, cloudy fluid expressed with more than moderate pressure; and grade 3, fluid cannot be expressed even with strong pressure.

• STATISTICAL ANALYSIS: All data are shown as the mean ± standard deviation. The Mann–Whitney *U* test was applied to the comparison between SS ATD and non-SS ATD groups in the examinations. A level of $P < .05$ was accepted as statistically significant. Graphpad Instat software version 3.0 (Graphpad Software, Inc, San Diego, California, USA) was used for statistical analysis.

RESULTS

• TEAR EVAPORATION RATES AND TEAR LIPID LAYER INTERFEROMETRY: Tear evaporation rates were 5.9 ± 3.5 (10^{-7} g/cm^2 per second) in the SS ATD group, which was significantly higher than the non-SS ATD group, 2.9 ± 1.8 (10^{-7} g/cm^2 per second; Table; $P = .0009$). The SS ATD group revealed DR-1 severity grading of 3.9 ± 1.2 (Figure, Left), which was significantly higher than DR-1 grading of the non-SS ATD group, 2.9 ± 1.1 (Figure, Right; $P = .03$).

• COMPARISON OF OCULAR SIGNS IN SS ATD AND NON-SS ATD GROUPS: The corneal fluorescein mean score was 3.0 ± 2.4 in the SS ATD group, which was significantly higher than the non-SS ATD group, 0.9 ± 1.6 (Table; $P = .002$). Similarly, the mean rose bengal score was 3.7 ± 2.6 in the SS ATD group, which was also significantly higher than in the non-SS ATD group, 1.9 ± 2.5 ($P = .01$). However, tear BUT (2.6 ± 1.7 seconds in the SS ATD group and 3.1 ± 2.6 seconds in the non-SS ATD group; $P = .95$) and Schirmer I test values (2.5 ± 2.0 mm in the SS ATD group and 2.0 ± 2.0 mm in the non-SS ATD group; $P = .3$) were not significantly different. Meibomian gland expressibility grading was 2.2 ± 0.4 in the SS ATD group, which was significantly higher than the non-SS ATD group, 1.0 ± 1.3 ($P = .04$).

DISCUSSION

IN THIS ARTICLE, WE REPORT TEAR EVAPORATION RATES IN SS ATD and the non-SS ATD groups. Tear evaporation rates were significantly higher in the SS ATD group compared with the non-SS ATD group, along with worse DR-1 severity grading, vital staining scores of the ocular surface, and meibomian gland expressibility grading (Table).

In the current study, tear evaporation rates were 5.9 ± 3.5 (10^{-7} g/cm^2 per second) and 2.9 ± 1.8 (10^{-7} g/cm^2 per second) in the SS ATD and the non-SS ATD groups, respectively. These results could be compared with those from our previous report about MGD (5.8 ± 2.7 [10^{-7} g/cm^2 per second]) and normal subjects (4.1 ± 1.4 [10^{-7} g/cm^2 per second]) using exactly the same evaporimeter setup.[11] Tear evaporation rates in the SS ATD group were close to those of the MGD subjects and were significantly higher than the normal subjects. Tear evaporation rates in the non-SS ATD group were significantly lower than normal subjects. As mentioned, tear evaporation rates, which were measured by our new ventilated chamber system,[11] in dry eyes with SS ATD, in dry eyes without SS ATD (this study), and also in eyes with MGD[11] showed similar trends to those reported in previous studies by our group using the closed chamber tear evaporimeter system.[9,10] However, as we pointed out in our previous report,[11] tear evaporation rates in ATD have been inconsistent in the literature. Rolando and associates and Mathers and associates, who used the modified closed chamber system, reported increased tear evaporation rates in ATD compared with normal subjects.[6,7] On the contrary, decreased tear evaporation rates in ATD have been reported by our group using the closed chamber tear evaporimeter system[10] and by Hamano and associates compared with normal subjects.[8] Because of these inconsistencies, we decided to examine the lipid layer status simultaneously with tear evaporimetry.

The difference in tear evaporation rates in ATD dry eye states could be explained by the observation of surface lipid layer status, which has been known to affect tear evaporation.[4,21] This lipid layer condition had been assumed by the observation of meibomian gland secretion at the lid margin.[9,13,22,23] However in this report, we observed the

tear surface lipid layer directly by using the DR-1 tear interference camera.

DR-1 severity grading in the present study was significantly higher in the SS ATD group (3.9 ± 1.2) compared with the non-SS ATD group (2.9 ± 1.1). DR-1 data showed increased dry eye severity grading in the SS ATD and the non-SS ATD groups compared with the previously reported data from normal subjects (1.5 ± 0.5).[12]

The representative DR-1 images from the SS ATD and the non-SS ATD groups are shown in the Figure, which revealed similar DR-1 grading, vital staining scores, tear BUT, and Schirmer I test values. However, tear evaporation rates were higher in the SS ATD group compared with the non-SS ATD group. Meibomian gland expressibility was worse and distribution of precorneal tear lipid was more uneven (lipid layer thickness range, 40 to 240 nm) in the SS ATD group compared with the non-SS ATD group in these representative cases. Such an uneven distribution and deficient lipid level on the upper cornea (Figure, Left) may result in higher tear evaporation rates in the SS ATD group compared with the non-SS ATD group.

However, it is also evident from the lipid layer thickness data that patients with non-SS ATD with better meibomian gland expressibility have a relatively more even distribution of lipid layer thickness over the cornea with a smaller range of thickness variation (Figure, Right; 120 to 220 nm). The non-SS ATD group had lower tear evaporation rates compared with the SS ATD group. Therefore, tear evaporation measurement when carried out with DR-1 may explain the difference in clinical findings.

For the evaluation of DR-1 tear interference images, the Yokoi severity grading system was used.[12,13] When we began the present study, a lipid layer thickness quantification system was not yet available. If we could have applied this system to all DR-1 images, the correlation between tear lipid layer thickness and tear evaporation might have been obtained more clearly. However, as we reported recently, the Yokoi severity grading system may be interpreted roughly as lipid layer thickness information as follows: grades 1 and 2, lipid layer thickness approximately 10 to 92.5 nm in dark to bright brownish-gray interference color; grade 3, lipid layer thickness from 100 to 185 nm in brown interference color; grade 4, lipid layer thickness from 190 nm to 370 nm in colorful interference images; and grade 5, no movement of interference image, indicating no lipid presence, lipid layer thickness approximately 0 nm.[24] Thus, we could judge tear lipid layer thickness condition from the Yokoi grading system. Furthermore, for the most recent data, a lipid layer thickness quantification system was applied.[14,24,25]

As shown in the Figure, analysis of distribution of precorneal tear lipid would be important, and the development of its index for the comparison of the data would be highly expected in future studies. Furthermore, in the future, tear evaporimtery of the other dry eye subtypes such as dry eyes with only decreased tear film BUT would be highly anticipated.[26]

In conclusion, we applied the new tear evaporimeter system to ATD dry eye states. Meibomian gland expressibility and precorneal lipid layer conditions examined by tear interferometry may explain the resultant tear evaporation rates in ATD dry eyes. This method can contribute to further understanding in the pathogenic mechanism of dry eyes and may give us clues for better treatment of dry eye patients.[27]

THIS STUDY WAS SUPPORTED BY GRANT NO.18070501 FROM THE JAPANESE MINISTRY OF HEALTH, LABOUR, AND WELFARE, Tokyo, Japan; Japanese patent application 2003-032898 (Drs Goto, Endo, and Tsuboto); and Japanese patent application 2003-032899 (Drs Endo and Tsuboto) for the evaporimeter set-up described herein as a "Tear Secretion Quantify Examination System." Drs Endo, Tsuboto, and Goto also have filed a US patent application on the method described herein and its clinical applications as "Tear Secretion Quantify Examination System." Drs Goto, Matsumoto, and Kamoi contributed equally to the work and therefore should be considered equivalent first authors. Involved in design of study (E.G., Y.M., M.K., R.I.); conduct of study (E.G., Y.M., M.K., K.E.); collection and analysis of the data (E.G., Y.M., K.E., R.I., M.K., T.K., K.T.); and approval of the manuscript (E.G., M.D., K.T.). The present research followed the tenets of the Declaration of Helsinki based on a protocol approved by the Institutional Review Board committee of Tokyo Dental College. Informed consent was obtained from all the subjects after explanation of the nature and possible consequences of the study. This clinical trial was registered to Japan Pharmaceutical Information Center (Tokyo, Japan, JapacCTI-060313).

The authors would like to thank Mr Hirayuki Sato, Analytical Research Center, KAO Corporation, Tochigi, Japan, Mr Atsushi Suzuki, Health Care Products Research Laboratories No. 2, KAO Corporation, Tokyo, Japan, and Naoshi Shinozaki, Executive Director, Cornea Center & Eye Bank, Tokyo Dental College, Chiba, Japan, for their instruction of the principles of the interference phenomena.

REFERENCES

1. Lemp MA. Report of the National Eye Institute/Industry Workshop on Clinical Trials in Dry Eyes. CLAO J 1995;21: 221–232.
2. Pflugfelder SC, Tseng SCG, Sanabria O, et al. Evaluation of subjective assessments and objective diagnostic tests for diagnosing tear-film disorders known to cause ocular irritation. Cornea 1998;17:38–56.
3. Driver PJ, Lemp MA. Meibomian gland dysfunction. Surv Ophthalmol 1996;40:343–367.
4. Tiffany JM. The lipid secretion of the meibomian glands. Adv Lipid Res 1987;22:1–62.
5. Mathers WD, Daley TE. Tear flow and evaporation in patients with and without dry eye. Ophthalmology 1996;103: 664–669.
6. Mathers WD, Binarao G, Petroll M. Ocular water evaporation and the dry eye. A new measuring device. Cornea 1993;12:335–340.
7. Rolando M, Refojo MF, Kenyon KR. Increased tear evaporation in eyes with keratoconjunctivitis sicca. Arch Ophthalmol 1983;101:557–558.

8. Hamano H, Hori M, Mitsunaga S. Application of an evaporimeter to the field of ophthalmology. J Jpn Contact Lens Soc 1980;22:101–107.
9. Shimazaki J, Goto E, Ono M, Shimmura S, Tsubota K. Meibomian gland dysfunction in patients with Sjögren syndrome. Ophthalmology 1998;105:1485–1488.
10. Tsubota K, Yamada M. Tear evaporation from the ocular surface. Invest Ophthalmol Vis Sci 1992;33:2942–2950.
11. Goto E, Endo K, Suzuki A, Fujikura Y, Matsumoto Y, Tsubota K. Tear evaporation dynamics in normal subjects and subjects with obstructive meibomian gland dysfunction. Invest Ophthalmol Vis Sci 2003;44:533–539.
12. Yokoi N, Takehisa Y, Kinoshita S. Correlation of tear lipid layer interference patterns with the diagnosis and severity of dry eye. Am J Ophthalmol 1996;122:818–824.
13. Yokoi N, Mossa F, Tiffany JM, Bron AJ. Assessment of meibomian gland function in dry eye using meibometry. Arch Ophthalmol 1999;117:723–729.
14. Goto E, Dogru M, Kojima T, Tsubota K. Computer-synthesis of an interference color chart of human tear lipid layer, by a colorimetric approach. Invest Ophthalmol Vis Sci 2003;44:4693–4697.
15. Fox RI, Saito I. Criteria for diagnosis of Sjögren's syndrome. Rheum Dis Clin North Am 1994;20:391–407.
16. Danjo Y. Diagnostic usefulness and cutoff value of Schirmer's I test in the Japanese diagnostic criteria of dry eye. Graefes Arch Clin Exp Ophthalmol 1997;235:761–766.
17. Goto E, Tseng SC. Differentiation of lipid tear deficiency dry eye by kinetic analysis of tear interference images. Arch Ophthalmol 2003;121:173–180.
18. Goto E, Tseng SC. Kinetic analysis of tear interference images in aqueous tear deficiency dry eye before and after punctal occlusion. Invest Ophthalmol Vis Sci 2003;44:1897–1905.
19. Toda I, Tsubota K. Practical double vital staining for ocular surface evaluation. Cornea 1993;12:366–367.
20. van Bijsterveld OP. Diagnostic tests in the Sicca syndrome. Arch Ophthalmol 1969;82:10–14.
21. Mishima S, Maurice DM. The oily layer of the tear film and evaporation from the corneal surface. Exp Eye Res 1961;1:39–45.
22. Shimazaki J, Sakata M, Tsubota K. Ocular surface changes and discomfort in patients with meibomian gland dysfunction. Arch Ophthalmol 1995;113:1266–1270.
23. Mathers WD. Ocular evaporation in meibomian gland dysfunction and dry eye. Ophthalmology 1993;100:347–351.
24. Goto E. Quantification of tear interference image: tear fluid surface nanotechnology. Cornea 2004;23:S20–S24.
25. King-Smith PE, Fink BA, Fogt N. Three interferometric methods for measuring the thickness of layers of the tear film. Optom Vis Sci 1999;76:19–32.
26. Toda I, Shimazaki J, Tsubota K. Dry eye with only decreased tear break-up time is sometimes associated with allergic conjunctivitis. Ophthalmology 1995;102:302–309.
27. Goto E, Dogru M, Fukagawa K, et al. Successful tear lipid layer treatment for refractory dry eye in office workers by low-dose lipid application on the full-length eyelid margin. Am J Ophthalmol 2006;142:264–270.

Biosketch

Eiki Goto, MD, is an Associate Professor of the Department of Ophthalmology, School of Dental Medicine, Tsurumi University, Japan. Dr Goto received his medical degree from the School of Medicine, Keio University, Japan and did his Research Fellow at Bascom Palmer Eye Institute, University of Miami, Miami, Florida. Dr Goto is affiliated with Japanese Cornea Society and Tear Film and Ocular Surface Society. Dr Goto's primary research interests are dry eye, tear interferometry, and lipid layer treatment.

Clinical and Experimental Immunology | ORIGINAL ARTICLE | doi:10.1111/j.1365-2249.2007.03448.x

Amelioration of lacrimal gland inflammation by oral administration of K-13182 in Sjögren's syndrome model mice

T. Nishiyama,*†‡ K. Mishima,* K. Obara,* H. Inoue,* T. Doi,‡ S. Kondo,‡ M. Saka,‡ Y. Tabunoki,‡ Y. Hattori,‡ T. Kodama,§ K. Tsubota¶ and I. Saito*

*Department of Pathology, Tsurumi University School of Dental Medicine, Yokohama, Japan, †Sjögren's Syndrome Project, Shinanomachi Research Park, Keio University, Tokyo, Japan, ‡Tokyo New Drug Research Laboratories II, Pharmaceutical Division, Kowa Co. Ltd, Tokyo, Japan, §Laboratory for Systems Biology and Medicine, Research Center for Advanced Science and Technology, Graduate School of Medicine, University of Tokyo, Tokyo, Japan, and ¶Department of Ophthalmology, School of Medicine, Keio University, Tokyo, Japan

Accepted for publication 29 May 2007
Correspondence: Ichiro Saito, Department of Pathology, Tsurumi University School of Dental Medicine, 2-1-3 Tsurumi, Tsurumi-ku, Yokohama, 230-8501, Japan.
E-mail: saito-i@tsurumi-u.ac.jp

Summary

Regulation of the adhesion of mononuclear cells to endothelial cells is considered to be a critical step for the treatment of inflammatory diseases, including autoimmune diseases. K-13182 was identified as a novel inhibitor for these adhesions. K-13182 inhibited the expression of vascular cell adhesion molecule-1 (VCAM-1, CD106) on human umbilical vein endothelial cells (HUVECs) and on mouse vascular endothelial cell line (MAECs) induced by tumour necrosis factor (TNF)-α. K-13182 also inhibited the adhesion of mononuclear cells to these HUVECs and MAECs, indicating that K-13182 suppressed these adhesions mediated by cellular adhesion molecules including VCAM-1. To evaluate the therapeutic effect in autoimmune disease model mice, K-13182 was orally administered to non-obese diabetic (NOD) mice as Sjögren's syndrome (SS) model mice. Severe destructive inflammatory lesions were observed in the lacrimal glands of vehicle-treated control mice; however, 8-week administration of K-13182 inhibited the mononuclear cell infiltration into the inflammatory lesions of the lacrimal glands. In K-13182-treated mice, the decrease in tear secretion was also prevented compared to the control mice. In addition, the apoptosis and the expression of FasL (CD178), perforin, and granzyme A was suppressed in the lacrimal glands of K-13182-treated mice. Therefore, K-13182 demonstrated the possibility of therapeutic efficacy for the inflammatory region of autoimmune disease model mice. These data reveal that VCAM-1 is a promising target molecule for the treatment of autoimmune diseases as a therapeutic strategy and that K-13182 has the potential as a new anti-inflammatory drug for SS.

Keywords: autoimmune disease, endothelial cells, lacrimal gland, NOD mouse, VCAM-1

Introduction

Sjögren's syndrome (SS) is an organ-specific autoimmune disorder characterized by lymphocytic infiltration and progressive loss of exocrine glands resulting in symptoms of dry mouth and dry eye due to insufficient secretion, and systemic production of autoantibodies to the ribonucleoprotein [1]. Although a large number of studies have been conducted [2–5], the mechanism of the destruction of the exocrine glands is still unclear.

In the first stage of inflammatory diseases, leucocytes migrate from the circulation into the sites in which inflammation manifests. Leucocyte adherence to the blood vessel wall through cell adhesion molecules is the important step for leucocyte migration [6]. When activated by inflammatory cytokines, endothelial cells express adhesion molecules such as vascular cell adhesion molecule-1 (VCAM-1), intercellular adhesion molecule-1 (ICAM-1, CD54) and E-selectin (CD62E). VCAM-1 is a cell surface glycoprotein which belongs to the immunoglobulin superfamily, and is adhesive to certain blood leucocytes and tumour cells that bear α4 integrins. In the vascular system, VCAM-1 is expressed on activated endothelial cells, smooth muscle cells and fibroblasts in a variety of pathological conditions, including atherosclerosis and inflammation [7–9]. These former studies indicate that endothelial/lymphocyte adhesion involving VCAM-1/VLA-4 (CD49d/CD29) control the migration of lymphocytes into the inflamed lesion. These cell adhesion molecules offer potential therapeutic targets to block the development of inflammation and tissue destruction.

In SS, it has been reported that the expression of cell adhesion molecules on vascular endothelial cells, such as ICAM-1 and VCAM-1, increased in the salivary and lacrimal glands [10]. In addition, these adhesion molecules play predominant roles in controlling T cell recruitment into these tissues and in the regulation of inflammation [11].

In this study, we identified the newly synthesized, low molecular weight compound K-13182, which inhibited the VCAM-1 expression on human umbilical vein endothelial cells (HUVECs), mouse aortic vascular endothelial cell lines (MAECs) and inhibited cellular adhesion between HUVECs and U-937 human monocytic cell lines. The purpose of this study is to evaluate the therapeutic effect of K-13182 and to clarify the mechanism in detail in SS model mice.

Materials and methods

Cell cultures

HUVECs were purchased from Clontech (Palo Alto, CA, USA), and cultured in EGM-2 medium (Clontech). Three or four time-passaged cells were used for the experiments. U-937 was obtained from American Type Culture Collection (Manassa, VA, USA) and maintained in RPMI-1640 medium containing 10% fetal calf serum (FCS) (Invitrogen, Carlsbad, CA, USA). Murine myeloid leukaemia cell line, WEHI-3, was obtained from Riken Cell Bank (Ibaraki, Japan) and maintained in RPMI-1640 medium containing 10% FCS and 2-mercaptoethanol. MAECs were isolated and established from p53-deficient mice in our previous study [12].The cells were maintained in M199 (Sigma, St Louis, MO, USA) supplemented with 5% FCS, 10 U/ml heparin sodium (Shimizu Pharmaceutical, Shizuoka, Japan), 100 U/ml penicillin (Invitrogen) and 100 μg/ml streptomycin (Invitrogen).

Expression of VCAM-1 on HUVECs and MAECs

The expression of VCAM-1 on MAECs and HUVECs was analysed with cell enzyme-linked immunosorbent assay (ELISA). MAECs and HUVECs (1×10^4) were seeded onto 96-well culture plates (Becton Dickinson, Franklin Lakes, NJ, USA). Confluent cultures of cells were stimulated with 10 ng/ml tumour necrosis factor (TNF)-α in the presence of various doses of K-13182. Non-specific binding was blocked by the sequential addition of 3% non-fat dry milk/phosphate-buffered saline (PBS) and 5% goat serum/PBS for 1 h. Anti-human VCAM-1 (4B2, Genzyme Corporation, Cambridge, MA, USA) or anti-mouse VCAM-1 (MK2·7, American Type Culture Collection) and horseradish peroxidase (HRP)-conjugated goat anti-rat IgG antibody (R&D Systems, Minneapolis, MN, USA) were used as the first and second antibodies, respectively, followed by the addition of 3, 3′, 5, 5′-tetramethyl-benzidine (Moss Inc., Pasadena, MD, USA). The optical density (OD) of each well was determined by using a microplate reader (Bio-Rad Laboratories, Hercules, CA, USA) at 450 nm. The relative VCAM-1 expression was calculated using the following formula: (expression in the presence of K-13182 [OD]/expression in the absence of K-13182 [OD]) × 100. Data are expressed as mean ± standard deviation (s.d.) of three individual experiments.

Cellular adhesion assay

Cellular adhesion assay using HUVECs or MAECs and U-937 or WEHI-3 was performed as described in previous reports [12–15], with some modifications. Endothelial cells (HUVECs or MAECs, 1×10^4/well) were seeded into each well of 96-well culture plates. Confluent cultures of endothelial cells were stimulated by 30 ng/ml TNF-α and varying concentrations of K-13182 for 16 h at 37°C. U-937 or WEHI-3 cells were labelled with 10 μmol/l 2′,7′-bis(carboxyethyl)-5(6′) carboxyfluorescein tetraacetoxymethyl ester (PKH-2; Dojindo Laboratories, Kumamoto, Japan) for 1 h at 37°C in each medium for HUVECs and MAECs and then washed three times with serum-free medium. PKH-2-labelled cells (2×10^4) were added to each well and incubated with TNF-α-stimulated endothelial cells for 1 h. Cells that were not bound to endothelial cells were removed by inverting the plates for 30 min. Wells were subsequently washed once with serum-free M199, and the remaining cells were lysed with 1% Nonidet P-40 (Calbiochem, La Jolla, CA, USA). Fluorescence intensity in cell lysate was measured by using an automated microplate fluorometer (Perkin Elmer, Boston, MA, USA) at an excitation wavelength of 485 nm and an emission wavelength of 535 nm. The relative adhesion cells were calculated using the following formula: (adhesion in the presence of K-13182 [OD]/adhesion in the absence of K-13182 [OD]) × 100.

Reverse transcription–polymerase chain reaction (RT–PCR) assay

MAECs and HUVECs were stimulated with 10 ng/ml TNF-α in the presence of K-13182 for 4 h. Total RNA was extracted with TRIzol reagent (Life Technologies, Rockville, MD, USA), and cDNA was prepared from RNA with 50 pmol of random hexamer and 200 U of reverse transcriptase (Invitrogen); 0·5 μl of a 20-μl cDNA mixture was used for PCR with 5 pmol each of forward and reverse primers and 2·5 U of Ex *Taq* DNA polymerase (Takara Shuzo, Kyoto, Japan). The sequences of the specific sense and anti-sense oligonucleotide primer pairs were as follows: VCAM-1 (human), GGATAATGTTTGCAGCTTCTC and TTCAGTAAGTC TATCTCCAGC; VCAM-1 (mouse), CCCAAGGATCCA GAGATTCA and TAAGGTGAGGGTGGCATTTC; β-actin, CTCTTTGATGTCACGCACGATTTC and GTGGGCCGC TCTAGGCACCAA.

Samples were amplified through 25 or 30 cycles in a PCR Thermal Cycler (Applied Biosystems, Foster City, CA, USA).

Mice

Male non-obese diabetic (NOD) mice were purchased from Clea Japan, Inc. (Tokyo, Japan) and maintained under specific-pathogen-free conditions in the animal facilities of Kowa Tokyo New Drug Research Laboratories. All experimental protocols were approved by the animal welfare committees of Tsurumi University and Kowa Tokyo New Drug Research Laboratories.

Administration of K-13182

K-13182, dissolved in 0·5% hydroxypropyl methylcellulose, was administered orally into the mice at a dose of 30 mg/kg/day from 4 to 12 weeks of age (8 week of administration, $n = 12$) or from 4 to 16 weeks of age (12 week of administration, $n = 15$). For control mice, 0·5% hydroxypropyl methylcellulose was administered as vehicle for a period of 8 ($n = 12$) or 12 weeks ($n = 15$).

Measurement of tear secretion

Tear secretion was compared before and after administration of K-13182. We measured the tear secretion of NOD mice before administration (control mice: $n = 5$; K-13182-treated mice: $n = 5$) and 12 weeks after administration (control mice: $n = 10$; K-13182-treated mice: $n = 11$). Mice were anaesthetized intraperitoneally with a mixture of 36 mg/kg ketamine (Sigma) and 16 mg/kg xylazine (Sigma). The amount of secreted tears was determined by the length of the Schirmer strip soaked by tears (1 mm in width; Showa Yakuhin Kako, Tokyo) after insertion into the inner aspect of an eyelid every 5 min in a 20-min period.

Histological analysis

NOD mice were anaesthetized with diethyl ether (Wako Pure Chemical Industries, Osaka, Japan) and were killed. The lacrimal glands were then removed from K-13182-treated NOD mice ($n = 11$, 8 weeks of administration, $n = 15$, 12 weeks of administration) and control mice ($n = 11$, 8 weeks of administration, $n = 15$, 12 weeks of administration). Removed lacrimal glands were fixed with 4% paraformaldehyde and embedded in paraffin. The sections (4 μm) were prepared and stained with haematoxylin and eosin (H&E) [16] using the standard method. Histological grading of the inflammatory lesions in the lacrimal glands was performed according to the method proposed by White and Casarett [17]. The number of mononuclear cells on H&E-stained sections (three areas/section/animal) obtained from each animal was counted under a light microscope (× 400), and the mean value was calculated for each animal.

*Taq*Man RT–PCR

Lacrimal glands were removed from NOD mice as mentioned above. Total RNA were obtained from the lacrimal glands of K-13182-treated mice or control mice. Reverse transcription was performed using a GeneAmp RNA PCR kit (Applied Biosystems). *Taq*Man–PCR was also performed according to the manufacturer's instructions (Applied Biosystems). Oligonucleotide primers and probes are described in Table 1. Sequence specific amplification was detected with an increased fluorescent signal of reporter dye 6-carboxy fluorescein (FAM) during the following amplification cycles: 1 cycle at 50°C for 2 min, 1 cycle at 95°C for 10 min and 40 cycles each at 95°C for 15 s and 60°C for 1 min. Gene-specific mRNA was normalized subsequently to rRNA. Primers and probes for rRNA were purchased from Applied Biosystems.

TUNEL assay

Lacrimal glands were removed from NOD mice, as mentioned above, and were embedded in optimal cutting temperature compound (OCT; Sakura Finetechnical, Tokyo, Japan) and frozen in liquid nitrogen. Cryostat sections (5 μm) were made, and apoptotic cells were detected in sections by terminal deoxynucleotidyl transferase-mediated dUTP nick end labelling (TUNEL) assay using the *in situ* apoptosis *in situ* detection kit (Wako Pure Chemical Industries), according to the manufacturer's instructions. The percentage of TUNEL-positive cells were counted under the light microscope (× 400) in three fields per one section (TUNEL index), and expressed as mean percentage ± s.d. in four (control mice) or three (K-13182-treated mice) sections.

Table 1. Primers and probes used for reverse transcription–polymerase chain reaction (RT–PCR) analysis.

mRNA	Sequences
VCAM-1	
Forward primer	ACAAGTCTACATCTCTCCCAGGAATAC
Reverse primer	CACAGCACCACCCTCTTGAA
Probe	CTGTACATCCCTCCACAAG
FasL	
Forward primer	TCAGCTCTTCCACCTGCAGAA
Reverse primer	TACTTTAAGGCTTTGGTTGGTGAA
Probe	AACTGGCAGAACTCCGT
Perforin	
Forward primer	GCAGGTCAGGCCAGCATAA
Reverse primer	ACCTTTGAATCCTGGCACTCA
Probe	AGTAGCCATGATTCATGCC
Granzyme A	
Forward primer	GGTGGAAAGGACTCCTGCAA
Reverse primer	GCCTCGCAAAATACCATCACA
Probe	ATTCTGGCAGCCCTC

Results

K-13182 inhibited cellular adhesion and the expression of VCAM-1 in HUVECs

In our previous study, the expression of VCAM-1, ICAM-1 and E-selectin on the HUVECs in response to TNF-α was augmented markedly [15]. Among these cell adhesion molecules, K-13182 suppressed VCAM-1 expression in a dose-dependent manner ($P < 0.0001$ at 0·01, 0·03, 0·1, 0·3 and 1 μM compared to absence of K-13182, Dunnett's multiple comparisons, Fig. 1a). The observed half-maximal inhibitory concentration (IC_{50}) for VCAM-1 expression was 0·019 μM. To examine the specificity of K-13182, ICAM-1 expression was also analysed by cell ELISA. K-13182 (0·1–10 μM) did not show a suppressive effect on ICAM-1 expression (Fig. 1b). Suppression of VCAM-1 expression was also confirmed at the transcriptional level using RT–PCR, and 1 μM of K-13182 clearly inhibited the VCAM-1 mRNA expression that was induced by 10 ng/ml TNF-α (Fig. 1d). These results demonstrated that K-13182 specifically inhibited VCAM-1 expression.

We have established a mononuclear cell/endothelial cell adhesion assay system for the functional analysis of adhesion inhibitory compounds in a former report [15]. To assess whether K-13182 can function in lymphocytic cellular adhesion to activated HUVECs, this cellular adhesion assay was performed in the presence of K-13182. HUVECs were treated with TNF-α (10 ng/ml) for 4 h in the presence of

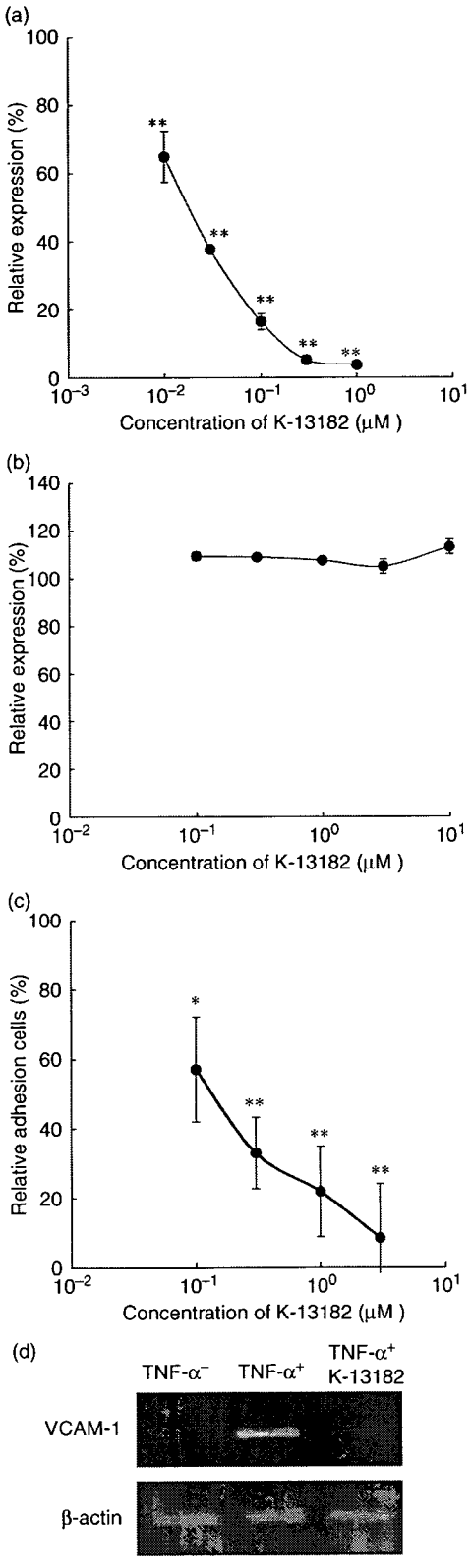

Fig. 1. The cell adhesion molecule expression and human mononuclear cell/endothelial cell adhesion. (a) Effects of K-13182 on vascular cell adhesion molecule-1 (VCAM-1) expression in human umbilical vein endothelial cells (HUVECs). HUVECs were stimulated with tumour necrosis factor (TNF)-α in the presence of K-13182 for 4 h. The expression of VCAM-1 was then investigated by cell enzyme-linked immunosorbent assay (ELISA). Data are expressed as percentage of control expression (without K-13182) and represented as mean ± s.d. of triplicate samples. Inhibitory concentration (IC_{50}) was 0·019 μM. Statistical analysis was made using Dunnett's multiple comparisons compared to absence of K-13182, $^{**}P < 0.001$. The results are the average of four separate experiments. (b) Effects of K-13182 on intercellular adhesion molecule-1 (ICAM-1) expression in HUVECs. ICAM-1 expression was not down-regulated by K-13182 in doses of 0–10 μM. (c) U-937/HUVECs adhesion assay. HUVECs were stimulated with TNF-α in the presence of K-13182 (0–3 μM) for 4 h. Adhesion of fluorescent-labelled U-937 cells were analysed by fluorescent spectrophotometer. IC_{50} was 0·14 μM. Data are expressed as percentage adhesion of cells added and represented as mean ± s.d. of triplicate samples. Statistical analysis was made using Dunnett's multiple comparisons compared to absence of K-13182, $^{*}P < 0.05$ and $^{**}P < 0.001$. (d) Effects of K-13182 on VCAM-1 mRNA expression in HUVECs. HUVECs were stimulated with 10 ng/ml TNF-α in the presence of 1 μM of K-13182 for 4 h. The expression of VCAM-1 was then investigated by reverse transcription–polymerase chain reaction (RT–PCR).

K-13182, and the cellular adhesion of U-937 cells to HUVECs was measured thereafter. As shown in Fig. 1c, the adhesion of U-937 to TNF-α-stimulated HUVECs was inhibited significantly by the treatment of K-13182 in a dose-dependent manner ($P < 0{\cdot}01$ at 0·1, 0·3, 1 and 3 μM compared to absence of K-13182, Dunnett's multiple comparisons). The observed IC_{50} for the cellular adhesion was 0·14 μM. Ten μM of K-13182 had no toxic effect on U-937 cells (data not shown).

K-13182 inhibited cellular adhesion and the expression of VCAM-1 in a murine endothelial cell line

We further confirmed the effects of K-13182 on a murine endothelial cell line. We used MAECs that had been established in our laboratory. Expression of VCAM-1 on MAECs was up-regulated in response to TNF-α stimulation and they retained cellular adhesion activity with WEHI-3 [12]. Stimulation with 10 ng/ml TNF-α showed a maximum VCAM-1 expression after 24 h (data not shown) and reached a plateau thereafter. We therefore decided to use a dose of TNF-α (10–30 ng/ml) for later experiments.

The expression of VCAM-1 on TNF-α-stimulated MAECs was significantly down-regulated by K-13182 in a dose-dependent manner ($P < 0{\cdot}001$ at 0·01, 0·03 and 0·1 μM compared to absence of K-13182, Dunnett's multiple comparisons, Fig. 2a). The IC_{50} for VCAM-1 expression in MAECs was 0·05 μM. Cell viability was assessed by the trypan blue dye exclusion test, and no cytotoxicity of K-13182 to MAECs was observed. K-13182 (0·3 μM) also suppressed the VCAM-1 expression that was up-regulated by

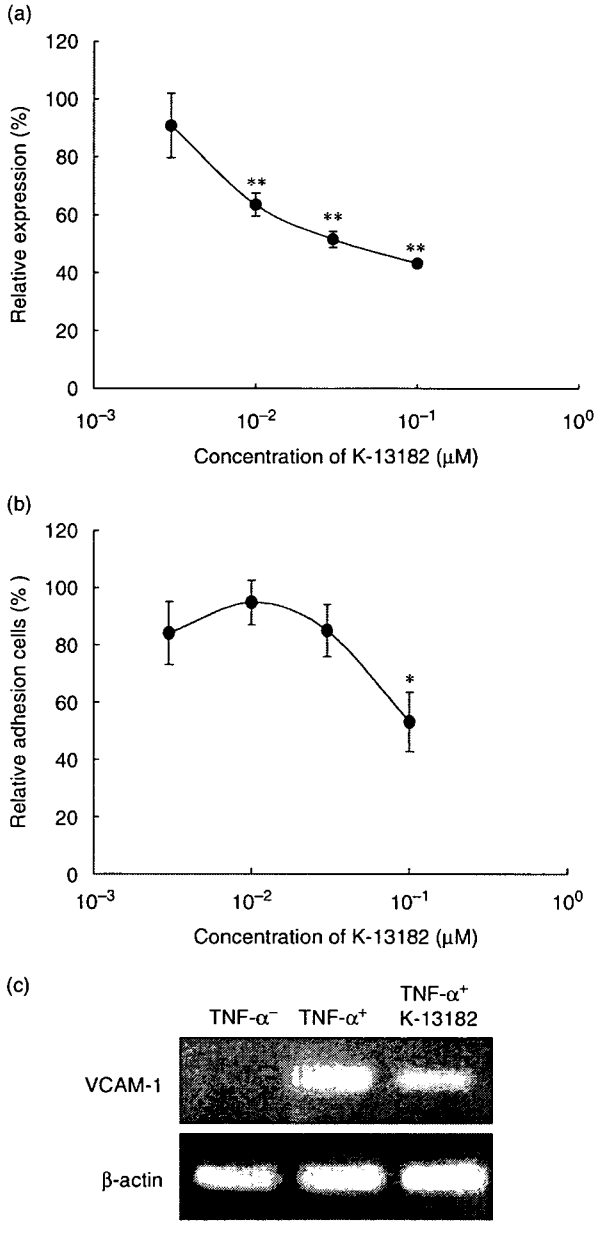

Fig. 2. Mouse vascular cell adhesion molecule-1 (VCAM-1) expression and mononuclear cell/endothelial cell adhesion. (a) Effects of K-13182 on the expression of VCAM-1 in mouse aortic vascular endothelial cell lines (MAECs). MAECs were stimulated with tumour necrosis factor (TNF)-α in the presence of K-13182 for 4 h. The expression of VCAM-1 was then investigated by cell enzyme-linked immunosorbent assay (ELISA). Inhibitory concentration (IC_{50}) was 0·05 μM. Data are expressed as percentage of control expression (without K-13182) and represented as mean ± s.d. of triplicate samples. Statistical analysis was made using Dunnett's multiple comparisons compared to absence of K-13182, $^{**}P < 0{\cdot}001$. (b) WEHI-3/MAECs adhesion assay. MAECs were pretreated with K-13182 (0–1·0 μM) overnight and stimulated with TNF-α for 4 h. Adhesion of fluorescent-labelled WEHI-3 cells was analysed by fluorescent spectrophotometer. IC_{50} was 0·10 μM. Data are expressed as percent adhesionage of cells added and represented as mean ± s.d. of triplicate samples. Statistical analysis was made using Dunnett's multiple comparisons compared to absence of K-13182, $^{*}P < 0{\cdot}05$. (c) Effects of K-13182 on VCAM-1 mRNA expression in MAECs. MAECs were stimulated with 10 ng/ml TNF-α in the presence of 0·3 μM of K-13182 for 4 h. The expression of VCAM-1 was then investigated by reverse transcription–polymerase chain reaction (RT–PCR).

10 ng/ml of TNF-α at the transcriptional level (Fig. 2c). There was more significant down-regulation of VCAM-1 mRNA in HUVECs and the concentration of K-13182 was 1 μM in HUVECs and 0·3 μM in MAECs. However, 1 μM of K-13182 did not show a significant effect compared with 0·3 μM of K-13182 in the RT–PCR in MAECs (data not shown).

To assess whether K-13182 affects mononuclear cellular adhesion with activated mouse endothelium, a cellular adhesion assay was performed using WEHI-3 and TNF-α-stimulated MAECs in the presence of K-13182. The adhesion of WEHI-3 to TNF-α-stimulated MAECs was inhibited significantly by the treatment with K-13182 in a dose-dependent manner ($P < 0{\cdot}05$ at 0·1 μM compared

to absence of K-13182, Dunnett's multiple comparisons, Fig. 2b). The IC_{50} for cellular adhesion assay was 0·10 μM.

Administration of K-13182 into NOD mice

The NOD mouse has been proposed as a valuable animal model for SS in humans, because NOD mice develop spontaneously mononuclear cell infiltration into the lacrimal and submandibular glands. Although diabetes developed only in female NOD mice, lymphocyte infiltration into the lacrimal glands was detected in male mice [18]. On the other hand, the destruction of submandibular glands was seen in female NOD mice [19]. Thus, we examined the *in vivo* therapeutic effects of K-13182 in male NOD mice as a murine model of lacrimal gland destruction. Body weight was monitored before (4·5 weeks of age) and after (16 weeks of age) administration of K-13182. Body weight increased in a time-dependent manner in both groups, and no statistical difference was detected between control and K-13182-treated mice at both 4·5 and 16 weeks of age (Fig. 3a). Side effects were not observed during administration of K-13182. In order to examine the anti-inflammatory effect of K-13182 in the lacrimal glands, they were analysed histologically after administration of K-13182. We evaluated their inflammatory lesions by the number of infiltrated mononuclear cells or inflammation score at 12 or 16 weeks of age, as described in the Materials and methods section. The number of infiltrated mononuclear cells in K-13182-treated mice was decreased significantly compared to control mice at 12 weeks of age ($P < 0·05$, Student's *t*-test). At 16 weeks of age it was also slightly decreased; however, statistical difference was not detected (Fig. 3b). So far, we do not have an explanation for this discrepancy between 12 and 16 weeks. Further analysis, including the subset of infiltrated lymphocytes, may be useful to analyse this. The inflammation score was slightly decreased in K-13182-treated mice; however, no statistical difference was detected at 12 and 16 weeks of age (data not

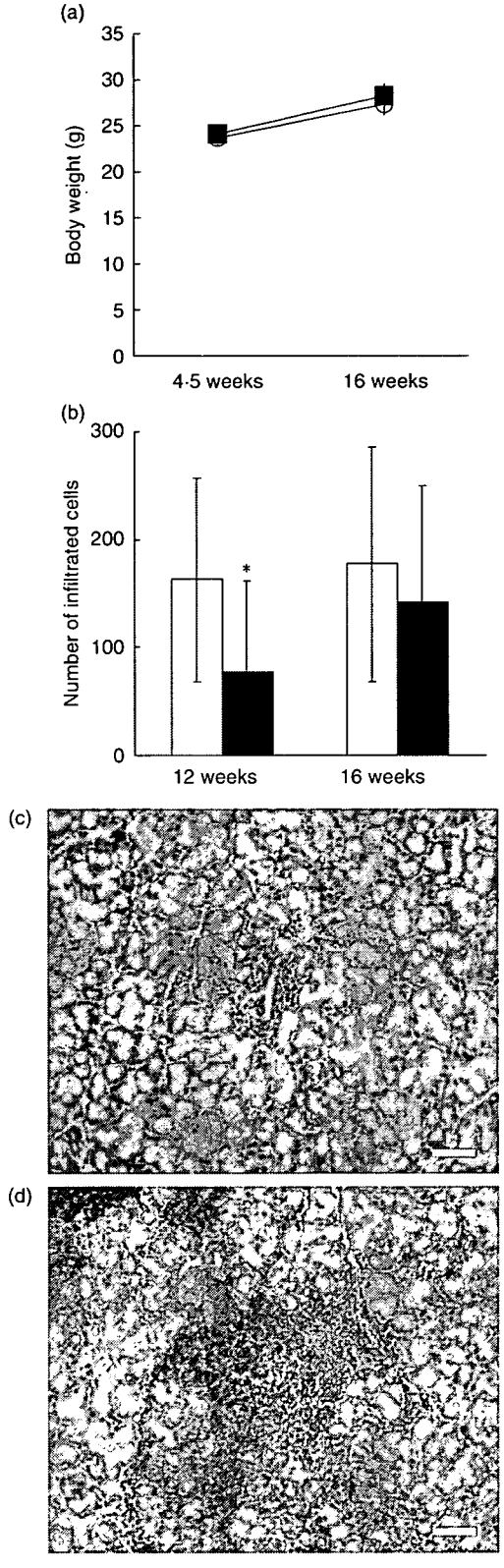

Fig. 3. Effects of *in vivo* administration of K-13182 in murine SS model. (a) The body weight of each mouse was measured at 4·5 weeks of age (control mice: open circle: $n = 5$; K-13182-treated mice: black square: $n = 5$) and at 16 weeks of age (control mice: $n = 10$; K-13182-treated mice: $n = 11$). Data are represented as mean ± s. d. of each time-point. (b) The number of infiltrated mononuclear cells in lacrimal glands at 12 weeks of age (control mice: $n = 12$; K-13182-treated mice: $n = 11$) was decreased significantly in K-13182-treated mice. Statistical difference was not detected at 16 weeks of age (control mice: $n = 14$; K-13182-treated mice: $n = 15$). The white and black bars indicate control mice and K-13182-treated mice, respectively. Data are represented as mean ± s.d. of each time-point. Statistical analysis was made using the Student's *t*-test, $^*P < 0·05$. Representative histological features showing severe lesions in the lacrimal glands in (c) control mice but not in (d) K-13182-treated mice. Original magnification ×200, scale bar 20 μm.

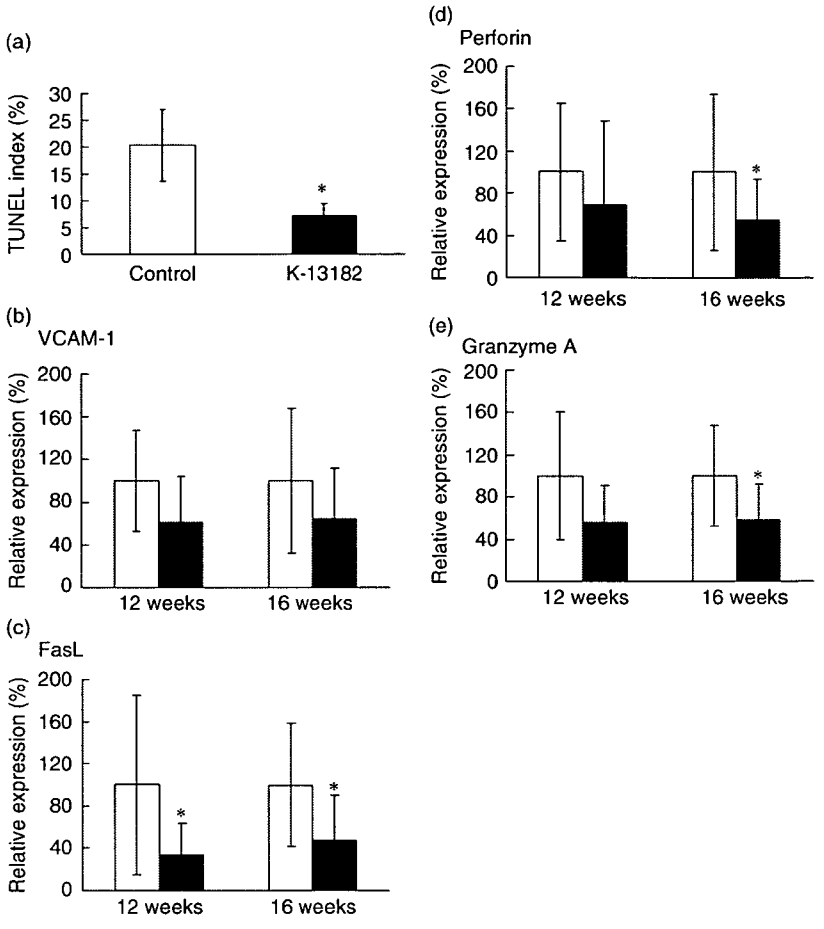

Fig. 4. Down-regulation of inflammatory molecules and apoptosis in K-13182-treated mice. (a) Apoptosis in K-13182-treated mice lacrimal glands was analysed at 12 weeks of age by terminal deoxynucleotidyl transferase-mediated dUTP nick end labelling (TUNEL) assay and the percentage of TUNEL-positive cells (TUNEL index) was measured. Data were analysed in three fields per one section, and were expressed as mean ± s. d. in four (control mice) or three (K-13182-treated mice) examined in each group. Down-regulated (c) FasL; (d) perforin; (e) granzyme A mRNA in K-13182-treated mice was examined at 12 and 16 weeks of age with real-time polymerase chain reaction (PCR). (b) Vascular cell adhesion molecule-1 (VCAM-1) was slightly down-regulated but statistical significance was not detected. rRNA is the internal control for the reverse transcriptase–PCR. The white and black bars indicate control mice and K-13182-treated mice, respectively. Statistical analysis was performed using Student's *t*-test, $^*P < 0{\cdot}05$.

shown). Representative histological features in the lacrimal glands are shown in Fig. 3c,d. These results revealed that treatment with oral administration of K-13182 (30 mg/kg/day) was effective in preventing the infiltration of mononuclear cells in the lacrimal glands of the SS model mice.

Tear secretion was also measured to analyse whether an anti-inflammatory effect led to the recovery or prevention of lacrimal gland dysfunction. Tear secretion was decreased significantly in control mice (34·7% decrease, $P < 0{\cdot}05$, Student's *t*-test) at 16 weeks of age compared to 4·5 weeks of age, while such a significant decrease was not shown in K-13182-treated mice at 16 weeks of age compared to 4·5 weeks of age (22·9% decrease, statistical difference was not detected). As tear secretion is decreased spontaneously in male NOD mice [20], this result demonstrated that K-13182 showed the preventive effect for tear decrease. As described previously, male NOD mice show mononuclear cell infiltration into only lacrimal glands; we therefore describe here the effect of K-13182 on the lacrimal glands. However, the effect of K-13182 on the pancreas and submandibular glands should be proved for further characterization of this compound.

Inhibition of apoptosis and apoptosis-related genes in lacrimal glands

Apoptosis of the acinar and ductal epithelial cells of the lacrimal glands has been proposed as a possible mechanism responsible for the impairment of secretory function in NOD mice [20,21]. In our study, decreased infiltration of mononuclear cells was demonstrated in K-13182-treated mice, as described above. From our results, we investigated the apoptosis in the lacrimal glands of NOD mice by TUNEL assay. Interestingly, the percentage of apoptotic cells was decreased in the lacrimal glands of K-13182-treated mice compared to control mice at 12 weeks of age (Fig. 4a; $P < 0{\cdot}05$, Student's *t*-test). In order to analyse the further anti-inflammatory mechanism of K-13182 in lacrimal glands, mRNA levels of FasL, perforin, granzyme A and VCAM-1 were measured by quantitative PCR. The mRNA of FasL ($P < 0{\cdot}05$, Fig. 4c) at 12 weeks of age, and FasL ($P < 0{\cdot}05$, Fig. 4c), perforin ($P < 0{\cdot}05$, Fig. 4d) and granzyme A ($P < 0{\cdot}05$, Fig. 4e) at 16 weeks of age were reduced significantly in K-13182-treated mice compared with control mice (Student's *t*-test). VCAM-1 was down-regulated slightly in K-13182-treated mice; however, statistical significance was not detected at 12 and

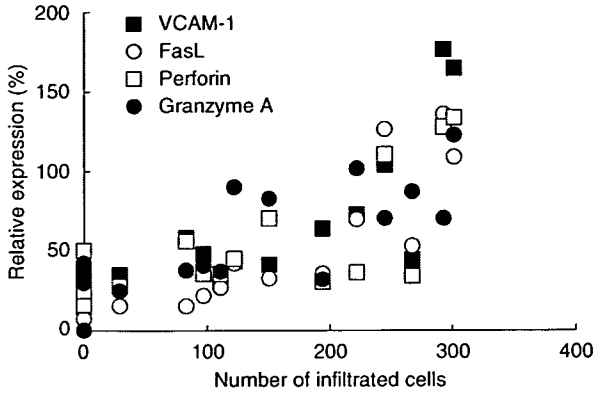

Fig. 5. Correlation coefficients between the number of infiltrated mononuclear cells and the results of quantitative polymerase chain reaction (PCR). Correlation coefficients (R^2) between the number of infiltrated mononuclear cells and the analysed gene mRNA levels were 0·59 [■: vascular cell adhesion molecule-1 (VCAM-1)], 0·74 (○: FasL), 0·46 (□ perforin) and 0·59 (●: granzyme A).

16 weeks of age (Fig. 4b). Correlation coefficients between the number of infiltrated mononuclear cells and the results of quantitative PCR were calculated to investigate the relation between the inflammation and expression of analysed genes in the lacrimal glands. As shown in Fig. 5, the expression of VCAM-1, FasL, perforin and granzyme A was proportional to the infiltrated mononuclear cell numbers at 16 weeks of age. Correlation coefficients (R^2) to infiltrated mononuclear cell number was 0·59 for VCAM-1, 0·74 for FasL, 0·46 for perforin and 0·59 for granzyme A.

Discussion

In the present study, our purpose was to assess the therapeutic effect of K-13182 as a therapeutic agent for SS *in vitro* and *in vivo*.

Regarding the inhibition of cellular adhesion of K-13182 between endothelial cells and mononuclear cells, as shown in *in vitro* experiments (Figs 1 and 2), K-13182 inhibited VCAM-1 expression in HUVECs and MAECs. In addition, cellular adhesion with endothelial cells and mononuclear cells was prevented in both human and murine co-culture assay systems. These results indicated that K-13182 retains the ability to inhibit mononuclear infiltration into the inflammatory region via endothelial cells, and the therapeutic effect shown in the *in vivo* analyses might be mediated by the prevention of cellular adhesion by K-13182.

Considering the effect of K-13182 on the VCAM-1 expression and cellular adhesion *in vitro*, IC_{50} for VCAM-1 expression was 0·019 μM (HUVECs) and 0·05 μM (MAECs), while IC_{50} for cellular adhesion was 0·14 μM (HUVECs) and 0·10 μM (MAECs). These results suggest that adhesion molecules other than VCAM-1 also contribute to cellular adhesion. Nakao *et al.* have shown that ICAM-1/β2 integrin also participated in the adhesion of U-937 cells on HUVECs [22]. In the VCAM-1 gene promoter region, functional transcription factor binding motifs have been reported, including nuclear factor (NF)-κB, interferon regulatory factor, AP-1 and GATA [23–27], while the ICAM-1 gene promoter also has SP-1, NF-κB and AP-1 binding sites; however, it does not contain the GATA binding motifs [28]. Taken together, K-13182 might have inhibited VCAM-1 but not ICAM-1 expression through the regulation of GATA in HUVECs and MAECs. Human VCAM-1 promoter region contains two conserved consensus binding sites for the GATA family, while the murine VCAM-1 promoter contains one site [29,30]. This number of GATA binding motifs may explain the smaller IC_{50} in HUVECs than in MAECs in VCAM-1 expression assays and cellular adhesion assays. K-13182 was developed from a compound (K-7174) that had shown an inhibitory effect for the GATA family [15]. However, details of the mechanisms regarding the inhibition of GATA and characteristics of K-13182 and K-7174 should be investigated in future study.

Following 12-week administration of K-13182, decreased infiltration of mononuclear cells to lacrimal glands was shown by histological analysis (Fig. 3b) and the preventive effect of K-13182 for tear decrease was also confirmed. These anti-inflammatory effects of K-13182 might be mediated by the down-regulation of VCAM-1 expression and mononuclear cell adhesion, considering the *in vitro* analyses (Figs 1 and 2). However, a statistically significant difference was not detected in the VCAM-1 expression in lacrimal glands of NOD mice (Fig. 4b). This discrepancy between the *in vitro* and *in vivo* experiments may be caused by the sample; we used endothelial cells in the *in vitro* experiment, while lacrimal glands used for quantitative PCR included various kind of cells. This sampling may lead to a slight suppression of VCAM-1 in K-13182-treated mice. Furthermore, the smaller IC_{50} of K-13182 for MAECs compared with the IC_{50} for HUVECs discussed above and the results of the RT–PCR (Figs 1d and 2c) may explain partly the low therapeutic efficacy including VCAM-1 mRNA expression in lacrimal glands in a mouse model. Although further investigation is needed to find in which cells K-13182 is effective in lacrimal glands, K-13182 is considered to contribute to the down-regulation of VCAM-1 expression and mononuclear cell infiltration in lacrimal glands because high correlation coefficients were detected between VCAM-1 expression and infiltrated cell number in K-13182-treated mice (Fig. 5).

Considering the decreased mononuclear infiltration in K-13182-treated mice lacrimal glands and proposed mechanism of apoptosis in NOD mice [20,21], we speculated that the apoptosis suppression that may be induced due to the reduced mononuclear cell infiltration via cell adhesion molecules including VCAM-1. TUNEL assay showed the decreased number of apoptotic cells in K-13182-treated mice lacrimal glands. Furthermore, quantitative PCR analysis in K-13182-treated mice lacrimal glands also

demonstrated the down-regulation of FasL, perforin and granzyme A, which are involved in SS [31–34]. Fas/FasL-mediated tissue destruction in SS lacrimal glands were also reported [31,32]. Granzyme A is a serine protease that is contained in the granules of activated lymphocytes and plays a role in the destruction of the SS lacrimal glands [33], and perforin was also reported to be expressed in the lacrimal glands of SS [34]. Taken together with our results, the prevention of the tear decrease in K-13182-treated mice can be explained partly by the suppression of apoptosis and molecules such as FasL, perforin and granzyme A that may be decreased due to the reduced mononuclear cell infiltration via cell adhesion molecules including VCAM-1.

Saito *et al.* determined that several cell adhesion molecules are involved in the lymphoid cell infiltration of salivary and lacrimal glands in SS patients [10]. Furthermore, previous studies have demonstrated that neutralizing monoclonal antibodies (mAb) of cell adhesion molecules prevented the development of experimental autoimmune encephalomyelitis in the murine model [35,36]. Therefore, the inhibition of signal transduction pathways involved in lymphocyte adhesion is also valuable in treating these autoimmune diseases. VCAM-1 plays a critical role in inflammatory reactions, from the original recruitment of leucocytes through successive steps in the continuing process [11]. In fact, VCAM-1/VLA-4 has been studied as a target for a variety of autoimmune diseases. The humanized mAb to alpha4 integrin, natalizumab, was approved recently in the United States for the treatment of relapsing multiple sclerosis [37]. Neutralizing mAb to VCAM-1 reduced clinical severity in collagen-induced arthritis in mice [38], and peptide inhibitor for VCAM-1 also prevented airway hyperresponsiveness in sheep [39]. Therefore, specific inhibitors of VCAM-1 induction in endothelial cells have been sought actively to develop a new therapeutic approach that would not elicit severe side effects in the case of the treatment of atherosclerosis or various chronic inflammatory disorders, including SS [40].

We have demonstrated here the potent effect of K-13182 in SS model mice, which might be caused by the preventive effect of cellular adhesion mediated by VCAM-1. Our results are consistent with a former report that showed antibodies against VCAM-1 almost completely blocked lymphocyte migration from the blood into inflamed lacrimal glands in NOD mice [18]. K-13182 showed similar effects on VCAM-1 expression and mononuclear adhesion both in murine and human endothelial cells. In this report, K-13182 was administered prior to disease onset for the prevention of the disease, therefore the therapeutic effect of K-13182 should be analysed further. However, from our results, K-13182 is a promising candidate for a SS therapeutic reagent.

Acknowledgements

The authors gratefully thank Roger E. Morgan for helpful comments and critical reading of the manuscript, Wakako Suzuki, Koichi Yamada, Aki Sato and Noriko Hitosugi for technical assistance, Naohiro Saito for maintenance of mice and Judith Nishino for helpful discussions during the preparation of this manuscript. This work was supported partially by grants-in-aid for scientific research from the Ministry of Education, Culture, Sports, Science and Technology of Japan. The Sjögren's syndrome Project of Keio University was supported by Kowa Co., Ltd.

References

1 Fox RI, Saito I. Criteria for diagnosis of Sjogren's syndrome. Rheum Dis Clin North Am 1994; 20:391–407.
2 Kang HI, Fei HM, Saito I *et al.* Comparison of HLA class II genes in Caucasoid, Chinese, and Japanese patients with primary Sjogren's syndrome. J Immunol 1993; **150**:3615–23.
3 Fox RI, Chilton T, Scott S, Benton L, Howell FV, Vaughan JH. Potential role of Epstein–Barr virus in Sjogren's syndrome. Rheum Dis Clin North Am 1987; 13:275–92.
4 Fox RI, Pearson G, Vaughan JH. Detection of Epstein–Barr virus-associated antigens and DNA in salivary gland biopsies from patients with Sjogren's syndrome. J Immunol 1986; **137**:3162–8.
5 Saito I, Servenius B, Compton T, Fox RI. Detection of Epstein–Barr virus DNA by polymerase chain reaction in blood and tissue biopsies from patients with Sjogren's syndrome. J Exp Med 1989; **169**:2191–8.
6 Springer TA. Traffic signals for lymphocyte recirculation and leukocyte emigration: the multistep paradigm. Cell 1994; **76**:301–14.
7 Nakashima Y, Raines EW, Plump AS, Breslow JL, Ross R. Upregulation of VCAM-1 and ICAM-1 at atherosclerosis-prone sites on the endothelium in the ApoE-deficient mouse. Arterioscler Thromb Vasc Biol 1998; **18**:842–51.
8 O'Brien KD, Allen MD, McDonald TO *et al.* Vascular cell adhesion molecule-1 is expressed in human coronary atherosclerotic plaques. Implications for the mode of progression of advanced coronary atherosclerosis. J Clin Invest 1993; **92**:945–51.
9 Morales-Ducret J, Wayner E, Elices MJ, Alvaro-Gracia JM, Zvaifler NJ, Firestein GS. Alpha 4/beta 1 integrin (VLA-4) ligands in arthritis. Vascular cell adhesion molecule-1 expression in synovium and on fibroblast-like synoviocytes. J Immunol 1992; **149**:1424–31.
10 Saito I, Terauchi K, Shimuta M *et al.* Expression of cell adhesion molecules in the salivary and lacrimal glands of Sjogren's syndrome. J Clin Lab Anal 1993; 7:180–7.
11 Nakajima H, Sano H, Nishimura T, Yoshida S, Iwamoto I. Role of vascular cell adhesion molecule 1/very late activation antigen 4 and intercellular adhesion molecule 1/lymphocyte function-associated antigen 1 interactions in antigen-induced eosinophil and T cell recruitment into the tissue. J Exp Med 1994; **179**:1145–54.
12 Nishiyama T, Mishima K, Ide F *et al.* Functional analysis of an established mouse vascular endothelial cell line. J Vasc Res 2007; **44**:138–48.
13 Kaneko M, Hayashi J, Saito I, Miyasaka N. Probucol downregulates E-selectin expression on cultured human vascular endothelial cells. Arterioscler Thromb Vasc Biol 1996; **16**:1047–51.
14 Kaneko M, Inoue H, Nakazawa R *et al.* Pirfenidone induces intercellular adhesion molecule-1 (ICAM-1) down-regulation on cultured human synovial fibroblasts. Clin Exp Immunol 1998; **113**:72–6.